

Counterion Condensation and Fluctuation-Induced Attraction

A.W.C. Lau¹ and P. Pincus²

¹*Department of Physics and Astronomy, University of Pennsylvania, Philadelphia, PA 19104*

²*Materials Research Laboratory, University of California, Santa Barbara, CA 93106-9530*

(Dated: March 22, 2022)

We consider an overall neutral system consisting of two similarly charged plates and their oppositely charged counterions and analyze the electrostatic interaction between the two surfaces beyond the mean-field Poisson-Boltzmann approximation. Our physical picture is based on the fluctuation-driven counterion condensation model, in which a fraction of the counterions is allowed to “condense” onto the charged plates. In addition, an expression for the pressure is derived, which includes fluctuation contributions of the whole system. We find that for sufficiently high surface charges, the distance at which the attraction, arising from charge fluctuations, starts to dominate can be large compared to the Gouy-Chapmann length. We also demonstrate that depending on the valency, the system may exhibit a novel first-order binding transition at short distances.

PACS numbers: 82.70.-y, 61.20.Qg

I. INTRODUCTION

Correlation effects may play an important role in controlling the structure and phase behavior of highly charged macroions in solutions [1]. The macroions may be charged membranes, stiff polyelectrolytes such as DNA, or charged colloidal particles. Recently, these effects have attracted a great deal of attention, since they may drastically alter the standard mean-field Poisson-Boltzmann (PB) picture [2, 3, 4, 5, 6]. For example, one surprising phenomenon is the *attraction* between two highly-charged macroions, as observed in experiments [7, 8, 9] and in simulations [10, 11, 12]. This attraction is not contained in the mean-field (PB) theory, even for an idealized system of two charged planar surfaces. Indeed, it has been proven that PB theory predicts only repulsion between like-charged macroions [13].

Very recently, another interesting effect that is not captured within the PB theory is predicted, namely the novel fluctuation-driven counterion condensation [14]. For a system consisting of a single charged surface and its oppositely charged counterions, Netz and Orland [5] showed that a simple perturbative expansion about the mean-field PB solution breaks down for sufficiently high surface charge. Thus, in this limit, fluctuation and correlation corrections can become so large that the solution to the PB equation is no longer a good approximation. To circumvent this difficulty, a *two-fluid* model was proposed in Ref. [14], in which the counterions are divided into a *free* and a *condensed* fraction. The free counterions have the usual 3D mean field spatial distribution, while the *condensed* counterions are confined to move only on the charged surface and thus effectively reduce its surface charge density. The number of condensed counterions is determined self-consistently, by minimizing the total free energy which includes *fluctuation* contributions. This theory predicts that if surface charge density of the plate is sufficiently high, a large fraction of counterions is “condensed” via a phase transition, similar to the liquid-gas transition with a line of first-order

phase transitions terminating at the critical point. Furthermore, the valence of the counterions plays a crucial role in determining the nature of the condensation transition. The physical mechanism leading to this counterion condensation is the additional binding arising from 2D charge-fluctuations, which dominate the system at high surface charge. In this paper, we extend this condensation picture to a system of two charged surfaces with their neutralizing counterions, and to study the electrostatic interaction between them.

Previous theoretical approaches to the problem of the attraction in charged surfaces includes both numerical and analytical methods that go beyond the mean-field PB theory. Gulbrand *et al.* [10] provides the first convincing demonstration for the attraction between highly-charged walls using Monte Carlo simulations. In particular, they showed that for *divalent* counterions, the pressure between charged walls becomes negative for distances less than 10 Å; Hence, the existence of short-ranged attraction. Subsequently, there has been a number of numerical studies based on the hypernetted chain integral equation [15] and the local density-functional theory [16], as well as analytic perturbative expansion around the PB solution [17] that demonstrate attraction.

More recently, motivated by the problems of DNA condensation and membrane adhesion, two distinct approaches have been proposed to account for the attraction arising from correlations [2, 3, 4]. The first approach based on “structural” correlations first proposed by Rouzina and Bloomfield [2], the attraction comes from the ground state configuration of the “condensed” counterions. This theory predicts a strong short-ranged attraction, with the characteristic length set by the lattice constant, typically of the order of few Angstroms. In the other approach, based on charge-fluctuations, the counterion fluctuations are approximated by the 2D Debye-Hückel theory, which predicts a long-ranged attraction which scales with the interplanar distance as d^{-3} . Note, however, that the mean-field PB repulsion which scales like d^{-2} always dominates the attraction for large dis-

tances, and thus, the range of the attraction in this picture is still short, typically of the order of 10 \AA [18, 19]. Despite of the fact that some conceptual issues have been resolved concerning the crossover of the attractions from long-ranged to short-ranged [20, 21], there remain some interesting problems to be understood. In particular, some experimental observations in planar surfaces [8] and in charged colloidal suspensions [9] as well as computer simulations [12] provide evidence for a long-ranged attraction, typically of the order of microns, whereas the two mechanisms mentioned above give only short-ranged attraction. In this paper, we show that the charge-fluctuation approach, together with the counterion condensation mechanism [14], can induce long-ranged attractions for sufficiently high surface charge. We note that other mechanisms based on hydrodynamic interactions [22], depletion effects [23], and an exact calculation for the 2D plasma model [24] have been proposed recently to account for the long-ranged attractions.

In particular, we study the interaction between two charged surfaces separated by a distance d , with counterions distributed both inside and outside of the gap. This boundary condition, as opposed to all of the counterions confined between the gap, is more appropriate in general, since systems are not closed and often the counterions are in equilibrium with a “bath” in surface forces experiments. In the spirit of the “two-fluid” model proposed in Ref. [14], we divide the counterions into a “condensed” and a “free” fraction. The condensed counterions are allowed to move only on the charged surfaces, while the free counterions distribute in the space inside and outside the gap. The surface density of the condensed counterion n_c on each plate is determined by minimizing the total free energy, which includes fluctuation contributions. Furthermore, an expression for the fluctuation pressure is derived, which includes fluctuation contributions from the condensed and “free” counterions, and their couplings. We find that the counterion condensation can occur either by increasing surface charge density at a fixed distance or by decreasing the separation between plates. For low surface charge, the counterion condensation proceeds continuously as a function of distance with the fraction of counterion condensed being small but finite, and the total pressure of the system remains repulsive.

For higher surface charges, the qualitative behavior of the counterion condensation transition depends critically on the valence Z of the counterions. For $Z < 2$, the counterion condensation proceeds continuously as a function of distance. On the other hand, for $Z \geq 2$, the behavior of the system is qualitatively different, similar to an isolated charged plate [14]. In this case, the counterion condensation occurs via a first-order phase transition as a function of distance. Remarkably, we find that for *trivalent* ($Z = 3$) counterions, there is a wide range in the surface density, in which the first-order counterion condensation spontaneously takes that the system from a repulsive regime to an attractive regime at short distances, resulting in a first-order binding transition. For

high surface charge, counterion condensation again proceeds continuously even for $Z \geq 2$, but with a significant number of condensed counterions. Thus, in this regime, the mean-field repulsion is substantially reduced and the long-ranged charge-fluctuation attraction dominates the system even for large distances. Note, however, that the mean-field repulsion will eventually dominate as $d \rightarrow \infty$. We emphasize that all these features, in particular the special role of the valence, deviate significantly from the PB mean-field predictions.

This paper is organized as follows: In Sec. II, we briefly recapitulate qualitatively the mechanism which drives the counterion condensation. In Sec. III, we present in detail the two-fluid model and derive a general expression for the total free energy of the counterions. In Sec. IV, we apply this formalism to study the interaction of similarly charged surfaces. A detailed discussion of our results is presented in Sec. V.

II. COUNTERION CONDENSATION: QUALITATIVE ARGUMENT

In this section, we recapitulate the essential physics of the condensation transition presented in Ref. [14]. Recall that for a single plate of charge density $\sigma(\mathbf{x}) = en_0\delta(z)$ immersed in an aqueous solution of dielectric constant ϵ , containing oppositely charged $-Ze$ point-like counterions of valence Z on both sides of the plate, PB theory predicts that the counterion distribution [25]

$$\rho_0(z) = \frac{1}{2\pi Z^2 l_B (|z| + \lambda)^2}, \quad (1)$$

decays to zero algebraically with a characteristic length $\lambda \equiv 1/(\pi l_B Z n_0)$, where $l_B \equiv \frac{e^2}{\epsilon k_B T} \approx 7 \text{ \AA}$ is the Bjerrum length in water at room temperature, k_B is the Boltzmann constant, and T is the temperature. This Gouy-Chapman length λ defines a sheath near the charged surface within which most of the counterions are confined. Typically, it is on the order of few angstroms for a moderate charge density of $n_0 \sim 1/100 \text{ \AA}^{-2}$. Note that since λ scales inversely with n_0 and linearly with T , at sufficiently high density or low temperature, the counterion distribution is essentially two-dimensional. In fact, in the limit $T \rightarrow 0$, we have

$$\lim_{T \rightarrow 0} \int_{-\zeta}^{\zeta} \rho_0(z) dz = \lim_{T \rightarrow 0} 2 \cdot \frac{n_0}{2Z} \cdot \frac{\zeta}{\lambda + \zeta} = \frac{n_0}{Z}, \quad (2)$$

where ζ is an arbitrarily small but fixed positive value of z , *i.e.* the counterion profile $\rho_0(z)$ reduces to a surface density coating the charged plane with a density of n_0/Z . Therefore, according to PB theory, all of the counterions collapse onto the charged plane at zero temperature. However, for highly charged surfaces $Z^2 l_B \gg \lambda$, the fluctuation corrections become so large that the solution to the PB equation is no longer valid [5]. To capture this regime in the spirit of the “two-fluid” model [14],

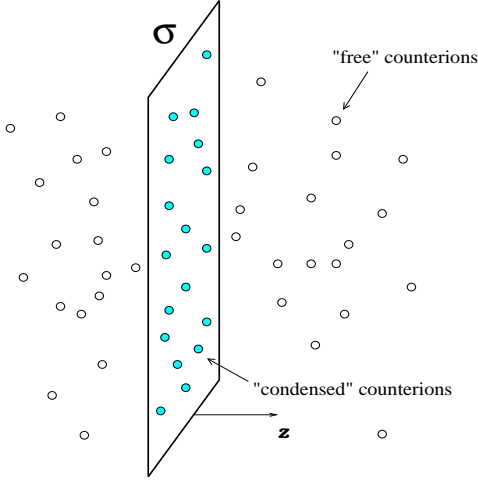


FIG. 1: The geometry of the problem.

we divide the counterions into a “free” and a condensate fraction. The “free” counterions have the usual PB 3D spatial distribution, while the “condensed” counterions are confined to move only on the charged plane, as shown in Fig. 1. The free energy per unit area for the condensed counterions with an average surface density n_c can be written as [26]

$$\beta f_{2d}(n_c) = n_c \{ \ln[n_c a^2] - 1 \} + \frac{1}{2} \int \frac{d^2 \mathbf{q}}{(2\pi)^2} \left\{ \ln \left[1 + \frac{1}{q \lambda_D} \right] - \frac{1}{q \lambda_D} \right\}, \quad (3)$$

where $\beta^{-1} = k_B T$, a is the molecular size of the counterions, and $\lambda_D = 1/(2\pi Z^2 n_c)$ is the 2D screening length. The first term in Eq. (3) is the entropy and the second term arises from the 2D fluctuations. Note that the latter term is logarithmically divergent, which may be regularized by a microscopic cut-off $\sim a$, yielding $\beta \Delta f_{2d}(n_c) \simeq -\frac{1}{8\pi \lambda_D^2} \ln(2\pi \lambda_D/a)$. In addition, the condensate partially neutralizes the charged plane, effectively reducing its surface charge density from en_0 to $en_R = en_0 - Z n_c$. Thus, motivated by PB theory, the free counterions can be modelled as an ideal gas confined to a slab of thickness $\lambda_R \equiv 1/(\pi l_B Z n_R)$ with a 3D concentration of $c = n_R/(Z \lambda_R)$. The fluctuation free energy in this case may be estimated using the 3D Debye-Hückel theory: $\beta \Delta f = -\kappa_s^3/(12\pi)$ [27], where $\kappa_s^2 = 4\pi Z^2 l_B c$ is the inverse square of the 3D screening length. The free energy per unit area of the free counterions is then approximately given by

$$\beta f_{3d}(n_c) \approx c \lambda_R \{ \ln[c a^3] - 1 \} - \frac{\kappa_s^3}{12\pi} \lambda_R. \quad (4)$$

All the qualitative results, including the nature of the condensation transition, follow straightforwardly from the analysis of the total free energy: $f(n_c) = f_{2d}(n_c) + f_{3d}(n_c)$; minimizing $f(n_c)$ to find the fraction of con-

densed counterions, n_c , we obtain

$$\ln \left[\frac{\tau}{(1-\tau)^2 \theta g} \right] + \frac{4}{3} g(1-\tau) - \tau g \ln \left(\frac{\pi}{\tau \theta g} \right) = 1, \quad (5)$$

where the three dimensionless parameters: the order parameter $\tau \equiv Z n_c/n_0$, the coupling constant $g \equiv Z^2 l_B/\lambda$, (where λ is the *bare* Gouy-Chapmann length), and the reduced temperature $\theta \equiv \frac{a}{Z^2 l_B}$, completely determine the equilibrium state of the system. It is easy to derive the asymptotic solutions of the last equation corresponding to the free, $\tau_1 \ll 1$, and condensed, $\tau_2 \approx 1$, state of the counterions: $\tau_1 \simeq g \theta \exp[1 - \frac{4}{3}g]$, and $\tau_2 \simeq 1 - [\pi \exp(1)]^{-1/2} \left(\frac{g \theta}{\pi} \right)^{\frac{g-1}{2}}$, respectively. For weak couplings $g \ll 1$, τ_1 is the only consistent solution. Thus, there is almost no condensed counterions $\tau \ll 1$. This is not surprising since PB theory is a weak-coupling theory which becomes exact in the limit $T \rightarrow \infty$. However, for high surface charge $g \gg 1$, where correlation effects becomes important, the behavior of τ depends crucially on θ . In particular, for $\theta < \theta_c \approx 0.038$, τ_1 and τ_2 are both consistent solutions corresponding to the two minima of f , and thus a first-order transition takes place when $f(\tau_1) = f(\tau_2)$, in which a large fraction of counterions is condensed. This occurs at a particular value of the bare surface charge density such that $g = g_0(\theta)$. For an estimate, we take $\theta = 0.02$ (divalent counterions at room temperature) and obtain $g_0 \sim 1.7$, corresponding to $\sigma_c \sim e/10 \text{ nm}^{-2}$. However, for $\theta > \theta_c$ the behavior of τ is completely different; in this regime, there is *no phase transition* and the condensation occurs continuously. Thus, the condensation transition is similar to the liquid-gas transition, which has a line of first-order transitions terminating at the critical point where a *second-order* transition occurs. If one takes $l_B \sim 10 \text{ \AA}$, *e.g.* room temperature, and $a \sim 1 \text{ \AA}$, it follows from the definition of θ that there is a critical value of counterion valence $Z_c = \sqrt{a/(l_B \theta_c)} \simeq 1.62$, below which no first-order condensation transition is possible. Therefore, divalent counterions behave *qualitatively* differently from monovalent counterions at room temperature.

Clearly, this condensation picture may also be crucial to understanding the attraction between two similarly charged plates, separated by a distance d . Recall that the total pressure of this system is comprised of the mean-field repulsion and the correlated fluctuation attraction [4]. The repulsion comes solely from the ideal gas entropy and it is proportional to the concentration at the mid-plane: $\Pi_0(d) = k_B T \rho_0(0) = 8k_B T/(\ell_B \lambda_R^2)$ for $d < \lambda_R$ [28]. The fluctuation-induced attraction is $\Pi(d) = -\alpha_0 k_B T/d^3$ for $d > \lambda_D$, where $\alpha_0 \approx 0.048$ [4]. Clearly, when a large fraction of the counterions is “condensed”, the mean-field repulsion is greatly reduced. Therefore, the attraction arising from correlated fluctuations of the “condensed” counterions can overcome the mean-field repulsion even for large distances. Using the estimates in the last paragraph above, we find that for *divalent* counterions and surface charge density of about

one unit charge per $\Sigma \sim 7 \text{ nm}^2$, the total pressure becomes attractive at about $d \sim 10 \text{ nm}$; hence a long-ranged attraction. Of course, this estimate should be supplemented by a more precise calculation for the system of two charged plates, which is done below.

III. COUNTERION FREE ENERGY IN THE “TWO-FLUID” MODEL

Consider an overall neutral system consisting of counterions and two charged surfaces separated by a distance d immersed in an aqueous solution. The surface charged density on each plate is $\sigma_0 = en_0$. We model the aque-

ous solution with a uniform dielectric constant ϵ . This simplification allows us to study fluctuation and correlation effects analytically. In the spirit of the “two-fluid” model proposed in Ref. [14], we divide the counterions into a “condensed” and a “free” fraction. The condensed counterions are allowed to move only on the charged surfaces, while the free counterions distribute in the space inside and outside the gap. The number of the condensed counterion n_c on each plate is determined by minimizing the total free energy including fluctuation contributions. Thus, our first task is to derive an expression for the total free energy of the system. The electrostatic free energy for the whole system may be written as

$$\begin{aligned} \beta F_{el} = & \sum_i \int d^2\mathbf{r} n_c^i(\mathbf{r}) \{ \ln [n_c^i(\mathbf{r}) a^2] - 1 \} + \int d^3\mathbf{x} \rho(\mathbf{x}) \{ \ln [\rho(\mathbf{x}) a^3] - 1 \} \\ & + \frac{Z^2 l_B}{2} \sum_{ij} \int d^3\mathbf{x} \int d^3\mathbf{x}' \frac{n_c^i(\mathbf{r}) \delta(z - z_i) n_c^j(\mathbf{r}') \delta(z - z_j)}{|\mathbf{x} - \mathbf{x}'|} + \frac{Z^2 l_B}{2} \int d^3\mathbf{x} \int d^3\mathbf{x}' \frac{\rho(\mathbf{x}) \rho(\mathbf{x}')}{|\mathbf{x} - \mathbf{x}'|} \\ & + Z l_B \sum_i \int d^3\mathbf{x} \int d^3\mathbf{x}' \frac{n_c^i(\mathbf{r}) \delta(z - z_i) [Z \rho(\mathbf{x}') - n_f(\mathbf{x}')] }{|\mathbf{x} - \mathbf{x}'|} - Z l_B \int d^3\mathbf{x} \int d^3\mathbf{x}' \frac{\rho(\mathbf{x}) n_f(\mathbf{x}')}{|\mathbf{x} - \mathbf{x}'|} \\ & + \frac{l_B}{2} \int d^3\mathbf{x} \int d^3\mathbf{x}' \frac{n_f(\mathbf{x}) n_f(\mathbf{x}')}{|\mathbf{x} - \mathbf{x}'|}, \end{aligned} \quad (6)$$

where a is the molecular size of the counterions, $l_B = e^2/(\epsilon k_B T)$ is the Bjerrum length, Z is the valence of the counterions, and $z_1 = -d/2$ and $z_2 = d/2$ are the locations of the charged surfaces. The first two terms in Eq. (6) are the two-dimensional entropy for the condensate and three-dimensional entropy for the “free” counterions, respectively, and the rest represent the electrostatic interactions of counterions in the system. In Eq. (6), the condensed counterions two-dimensional density on the i -th plate is denoted by $n_c^i(\mathbf{r})$, the “free” counterions with 3D density by $\rho(\mathbf{x})$, and the external fixed charges arising from the surfaces by $n_f(\mathbf{x}) = n_0 \delta(z - d/2) + n_0 \delta(z + d/2)$. Within the Gaussian fluctuation approximation, we assume that the 2D density of condensed counterions has a spatially dependent fluctuation about a uniform mean: $n_c^i(\mathbf{r}) = n_c + \delta n_c^i(\mathbf{r})$, and expand Eq. (6) to second order in $\delta n_c^i(\mathbf{r})$. Summing over all the 2D fluctuations of the condensed counterions, *i.e.*

$$e^{-\beta \mathcal{H}_e} = \int \mathcal{D} \delta n_c^A(\mathbf{r}) \mathcal{D} \delta n_c^B(\mathbf{r}) e^{-\beta F_{el}},$$

we obtain two terms in the effective free energy: $\mathcal{H}_e = F_{2d} + \mathcal{H}_{3d}$. The first term F_{2d} is the free energy associated with the condensed counterions which can be written as

$$\beta F_{2d} = 2n_c \{ \ln [n_c a^2] - 1 \} \mathcal{A} + \frac{1}{2} \ln \det \hat{\mathbf{K}}_{2d}$$

$$- \frac{1}{2} \ln \det [-\nabla_{\mathbf{x}}^2], \quad (7)$$

where $\hat{\mathbf{K}}_{2d}(\mathbf{x}, \mathbf{y}) \equiv \left[-\nabla_{\mathbf{x}}^2 + \frac{2}{\lambda_D} \sum_{\pm} \delta(z \pm d/2) \right] \delta(\mathbf{x} - \mathbf{y})$ is the 2D Debye-Hückel operator and $\lambda_D = 1/(2\pi Z^2 l_B n_c)$ is the Debye screening length in 2-D. The first term in Eq. (7) is the entropy and the second term arises from the 2D charge-fluctuations. Note that although this fluctuation term can be evaluated analytically [4], we write it in this abstract form for later convenience.

The second term \mathcal{H}_{3d} is the electrostatic free energy for the “free” counterions, taking into account of the presence of the fluctuating condensate; to within an additive constant, it may be written as

$$\begin{aligned} \beta \mathcal{H}_{3d} = & \int d^3\mathbf{x} \rho(\mathbf{x}) \{ \ln [\rho(\mathbf{x}) a^3] - 1 \} \\ & + \frac{1}{2} \int d^3\mathbf{x} \int d^3\mathbf{x}' \rho(\mathbf{x}) G_{2d}(\mathbf{x}, \mathbf{x}') \rho(\mathbf{x}') \\ & - \int d^3\mathbf{x} \phi(\mathbf{x}) \rho(\mathbf{x}), \end{aligned} \quad (8)$$

where $\phi(\mathbf{x}) \equiv \int d^3\mathbf{x}' Z^{-1} G_{2d}(\mathbf{x}, \mathbf{x}') n_R(\mathbf{x}')$ is the “renormalized” external field arising from the charged plate. From Eq. (8), we can see that the presence of the condensate modifies the electrostatics of the free counterions in

two ways. First, the condensate partially neutralizes the charged surfaces, effectively reducing the surface charge density from en_0 to $en_R = e(n_0 - Zn_c)$. Second, their fluctuations renormalize the electrostatic interaction of the system; thus, instead of the usual Coulomb potential, the free counterions and the charged surfaces interact via the interaction $G_{2d}(\mathbf{x}, \mathbf{x}')$, which is the inverse (the Green's function) of the 2D Debye-Hückel operator $\hat{\mathbf{K}}_{2d}$:

$$\left[-\nabla_{\mathbf{x}}^2 + \frac{2}{\lambda_D} \sum_{\pm} \delta(z \pm d/2) \right] G_{2d}(\mathbf{x}, \mathbf{x}') = \ell_B \delta(\mathbf{x} - \mathbf{x}'), \quad (9)$$

where we have defined, for convenience, a reduced Bjerrum length by $\ell_B \equiv 4\pi Z^2 l_B$. In Eq. (9), the second term in the bracket takes into account of the fluctuating “condensate”. Hence, in the limit $n_c \rightarrow 0$ or $\lambda_D \rightarrow \infty$, $G_{2d}(\mathbf{x}, \mathbf{x}')$ reduces to the usual Coulomb interaction $G_0(\mathbf{x}, \mathbf{x}') = \ell_B/|\mathbf{x} - \mathbf{x}'|$.

After a Hubbard-Stratonovich transformation [29], the grand canonical partition function for the “free” counterions, characterized by the interaction energy in Eq. (8), can be mapped onto a functional integral representation: $\mathcal{Z}_\mu[\phi] = \mathcal{N}_0 \int \mathcal{D}\psi e^{-\mathcal{S}[\psi, \phi]}$ with an action [30]

$$\begin{aligned} \mathcal{S}[\psi, \phi] = & \int \frac{d^3\mathbf{x}}{\ell_B} \left\{ \frac{1}{2} \psi(\mathbf{x}) [-\nabla^2] \psi(\mathbf{x}) - \kappa^2 e^{i\psi(\mathbf{x}) + \phi(\mathbf{x})} \right. \\ & \left. + \frac{1}{\lambda_D} \sum_{\pm} \delta(z \pm d/2) [\psi(\mathbf{x})]^2 \right\}, \end{aligned} \quad (10)$$

where $\psi(\mathbf{x})$ is the fluctuating field, $\kappa^2 = e^\mu \ell_B / a^3$, μ is the chemical potential and $\mathcal{N}_0^{-2} \equiv \det \hat{\mathbf{K}}_{2d}$ is the nor-

malization factor. The minimum of the action, given by $\left. \frac{\delta \mathcal{S}}{\delta \psi(\mathbf{x})} \right|_{\psi=\psi_0} = 0$, defines the saddle-point equation for $\psi_0(\mathbf{x})$

$$-\nabla^2[i\psi_0(\mathbf{x})] + \frac{2}{\lambda_D} \sum_{\pm} \delta(z \pm d/2) [i\psi_0(\mathbf{x})] + \kappa^2 e^{i\psi_0(\mathbf{x}) + \phi(\mathbf{x})} = 0. \quad (11)$$

This saddle-point equation is equivalent to the PB equation by defining the mean-field potential $\varphi(\mathbf{x}) = -i\psi_0(\mathbf{x}) - \phi(\mathbf{x})$, which is solved below in Sec. IV. To obtain the free energy for the free counterions on the mean-field level, we note that it is related to the Gibbs potential $\Gamma_0[\phi] \equiv \mathcal{S}[\psi_0, \phi]$ by a Legendre transformation:

$$\beta F_{3d}^0(n_R) = \Gamma_0[\phi] + \mu \int d^3\mathbf{x} \rho_0(\mathbf{x}), \quad (12)$$

where $\rho_0(\mathbf{x})$ is the mean-field free counterion density given by

$$\rho_0(\mathbf{x}) = (\kappa^2 / \ell_B) e^{i\psi_0(\mathbf{x}) + \phi(\mathbf{x})}. \quad (13)$$

To capture correlation effects, we must also include fluctuations of the “free” counterions, thereby treating the “free” and “condensed” counterions on the same level. To this end, we expand the action $\mathcal{S}[\psi, \phi]$ about the saddle-point $\psi_0(\mathbf{x})$ to second order in $\Delta\psi(\mathbf{x}) = \psi(\mathbf{x}) - \psi_0(\mathbf{x})$:

$$\mathcal{S}[\phi, \psi] = \mathcal{S}[\phi, \psi_0] + \frac{1}{2} \int d^3\mathbf{x} \int d^3\mathbf{y} \Delta\psi(\mathbf{x}) \hat{\mathbf{K}}_{3d}(\mathbf{x}, \mathbf{y}) \Delta\psi(\mathbf{y}) + \dots,$$

where the differential operator

$$\hat{\mathbf{K}}_{3d}(\mathbf{x}, \mathbf{y}) \equiv \left[-\nabla_{\mathbf{x}}^2 + \frac{2}{\lambda_D} \sum_{\pm} \delta(z \pm d/2) + \kappa^2 e^{i\psi_0(\mathbf{x}) + \phi(\mathbf{x})} \right] \delta(\mathbf{x} - \mathbf{y}), \quad (14)$$

is the second variation of the action $\mathcal{S}[\psi, \phi]$. Note that the linear term in $\Delta\psi(\mathbf{x})$ does not contribute to the expansion since $\psi_0(\mathbf{x})$ satisfies the saddle-point equation Eq. (11). Performing the Gaussian integrals in the functional integral, we obtain an expression for the change in the free energy due to fluctuations of the free counterions:

$$\beta \Delta F_{3d} = \frac{1}{2} \ln \det \hat{\mathbf{K}}_{3d} - \frac{1}{2} \ln \det \hat{\mathbf{K}}_{2d}, \quad (15)$$

where the second term comes from the normalization factor \mathcal{N}_0 . Note that the second term in Eq. (15) partially cancels the fluctuation contributions to the free energy of the condensed counterions in Eq. (7). Thus, combining Eqs. (7), (12), and (15) together, the total free energy of the system can be expressed as

$$\begin{aligned} \beta F(n_c) = & 2n_c \{ \ln[n_c a^2] - 1 \} \mathcal{A} + \beta F_{3d}^0(n_R) \\ & + \frac{1}{2} \ln \det \hat{\mathbf{K}}_{3d} - \frac{1}{2} \ln \det [-\nabla_{\mathbf{x}}^2]. \end{aligned} \quad (16)$$

This is the main result of this paper, from which all the equilibrium quantities can be calculated. It says that the free energy of the counterions is simply a sum of the mean-field free energy and a fluctuation energy term. Note that the latter term contains couplings among the fluctuations of the free and the condensed counterions. Finally, we stress that the derivation presented here is rather general and may apply to other physical systems as well.

IV. INTERACTION BETWEEN TWO SIMILARLY CHARGED SURFACES

In this section, we employ the framework of counterion condensation derived in Sec. III to study the interaction of two charged surfaces with free counterions and condensed counterions fluctuating on each of them. In Sec. IV A, an expression is derived for the total pressure, which takes into account the total fluctuations of the counterions. In Sec. IV B, we discuss the behavior of the total pressure and the equilibrium state of the system as characterized by the fraction of condensed counterion τ which is determined by the minimum of the total free energy Eq. (16).

A. Mean-Field Theory and Fluctuation Corrections

The free counterion density on the mean-field level can be obtained by solving Eq. (11). Defining the mean-field potential by $\varphi(\mathbf{x}) = -i\psi_0(\mathbf{x}) - \phi(\mathbf{x})$, the saddle-point equation becomes

$$\frac{d^2\varphi(z)}{dz^2} + \kappa^2 e^{-\varphi(z)} = \frac{n_R \ell_B}{Z} \sum_{\pm} \delta(z \pm d/2) + \frac{2}{\lambda_D} \sum_{\pm} \delta(z \pm d/2) \varphi(z), \quad (17)$$

where $en_R = e(n_0 - Zn_c)$ is the *renormalized* surface charge density of the plates. Note that Eq. (17) looks similar to the mean-field PB equation. Indeed, the solution to Eq. (17) is exactly the same as the PB solution provided that we impose the boundary condition: $\varphi(\pm d/2) = 0$. The solution reads

$$\varphi_{<}(z) = \ln \frac{\kappa^2 \cos^2(\alpha z)}{2\alpha^2}, \quad |z| \leq d/2, \quad (18)$$

$$\varphi_{>}(z) = 2 \ln \left[1 + \frac{\kappa}{\sqrt{2}} (|z| - d/2) \right], \quad |z| \geq d/2, \quad (19)$$

and the counterion density is given by

$$\rho_0 e^{-\varphi_{<}(z)} = (2\alpha^2/\ell_B) \sec^2(\alpha z), \quad |z| \leq d/2, \quad (20)$$

$$\rho_0 e^{-\varphi_{>}(z)} = \frac{2/\ell_B}{(|z| - d/2 + \xi)^2}, \quad |z| \geq d/2, \quad (21)$$

where $\xi \equiv \sqrt{2}/\kappa$ and α is determined from the boundary conditions on the electric field: $\partial_z \varphi_{>}|_{d/2} - \partial_z \varphi_{<}|_{d/2} = n_R \ell_B / Z$ and $\varphi(\pm d/2) = 0$; they lead to a transcendental equation for α :

$$\alpha \lambda_R \tan(\alpha d/2) = 1 - (\alpha \lambda_R / 2)^2, \quad (22)$$

where $\lambda_R = 4Z/(\ell_B n_R)$ is the *renormalized* Gouy-Chapmann length. Physically, α^2 is proportional to the free counterion density at the mid-plane $\rho_0(0)$. In addition, κ is related to the zeros of the potential, *i.e.* $\varphi(\pm d/2) = 0$:

$$\kappa^2 = 2\alpha^2 \sec^2(\alpha d/2) = 2(1 + b^2)^2 / \lambda_R^2, \quad (23)$$

where we have defined $b \equiv \alpha \lambda_R / 2$. The asymptotic behaviors for b as determined by the relation Eq. (22) are $b \sim 1/d$ as $d \rightarrow \infty$ and $b \sim 1$ as $d \rightarrow 0$. We note that the latter behavior is distinct from the case of two impenetrable charged hard walls [25].

The mean-field free energy per unit area for the free counterions, *i.e.*, the first two terms in Eq. (16), can be easily calculated by using Eq. (12),

$$\begin{aligned} \beta f_0 = & 2n_c \{ \ln[n_c a^2] - 1 \} + \frac{2n_R}{Z} \left\{ \ln \left(\frac{n_R a^3}{2Z \lambda_R} \right) - 1 \right\} \\ & + \frac{4n_R}{Z} \ln \left[1 + (\alpha \lambda_R / 2)^2 \right] + \frac{2\alpha^2 d}{\ell_B}, \end{aligned} \quad (24)$$

where we have made use of the fact that the chemical potential is given by $\mu = \ln(\kappa^2 a^3 / \ell_B)$. The first two terms in Eq. (24) represent the entropy per unit area of condensed and free counterions, respectively. The last two terms describe the interacting free energy for the surfaces. Using the general formula for the pressure: $\Pi_0(d) = -\frac{\partial f_0(d)}{\partial d}$, we obtain the mean-field pressure between the surfaces: $\Pi_0(d) = +2\alpha^2/\ell_B$. We note that at the mean-field level, the pressure comes solely from the ideal gas entropy of the “free” counterions, and it is proportional to their density at the midplane, a standard result. However, in contrast to the standard PB theory, the pressure now depends on the order parameter $\tau \equiv Zn_c/n_0$. Thus, if there were a large fraction of condensed counterions, $\tau \simeq 1$, the mean-field repulsion would be drastically reduced.

Next, we compute the pressure arising from the counterion fluctuations. Recall that the expression for the change in the free energy arising from fluctuations of the counterions is given by the last two terms in Eq. (16)

$$\beta \Delta \mathcal{F} = \frac{1}{2} \ln \det \hat{\mathbf{K}}_{3d} - \frac{1}{2} \ln \det [-\nabla_{\mathbf{x}}^2], \quad (25)$$

where the operators $\hat{\mathbf{K}}_{3d}$ is defined in Eq. (14) with

$$\kappa^2 e^{-\varphi(z)} = 2\alpha^2 \sec^2(\alpha z) \Theta(z) + \frac{2\tilde{\Theta}(z)}{(|z| - d/2 + \xi)^2}, \quad (26)$$

where $\xi \equiv \lambda_R/(1+b^2)$, $\Theta(z) = \theta(z+d/2) - \theta(z-d/2) = 1$, if $|z| \leq d/2$ and zero, otherwise, and $\tilde{\Theta}(z) = 1 - \Theta(z)$.

The derivative of $\Delta\mathcal{F}$ with respect to distance d can be straightforwardly calculated by making use of the exact identity: $\delta \ln \det \hat{\mathbf{X}} = \text{Tr} \hat{\mathbf{X}}^{-1} \delta \hat{\mathbf{X}}$,

$$\frac{\partial \beta \Delta \mathcal{F}}{\partial d} = \frac{1}{2\ell_B} \int d^3 \mathbf{x} G_{3d}(\mathbf{x}, \mathbf{x}) \times \frac{\partial}{\partial d} \left[\frac{2}{\lambda_D} \sum_{\pm} \delta(z \pm d/2) + \kappa^2 e^{-\varphi(z)} \right], \quad (27)$$

where $G_{3d}(\mathbf{x}, \mathbf{x}')$ is the Green's function of the operators $\hat{\mathbf{K}}_{3d}$ satisfying

$$\left[-\nabla_{\mathbf{x}}^2 + \frac{2}{\lambda_D} \sum_{\pm} \delta(z \pm d/2) + \kappa^2 e^{-\varphi(z)} \right] G_{3d}(\mathbf{x}, \mathbf{x}') = \ell_B \delta(\mathbf{x} - \mathbf{x}'). \quad (28)$$

An explicit derivation of $G_{3d}(\mathbf{x}, \mathbf{x}')$ and the pressure arising from fluctuations Eq. (27) are detailed in Appendix A. The final result for the pressure can be written as

$$\beta \Pi(d) = -\frac{1}{\mathcal{A}} \frac{\partial \Delta \mathcal{F}}{\partial d} = - \int \frac{d^2 \mathbf{q}}{(2\pi)^2} \frac{q \mathcal{M}^2(q)}{1 - \mathcal{M}^2(q)} - \frac{\alpha^2}{\lambda_R} \frac{(1 + b^2)(\mathcal{I}_2 - \mathcal{I}_3)}{2 + \frac{d}{\lambda_R}(1 + b^2)}, \quad (29)$$

where $\mathcal{M}(q)$ is defined in Eq. (A14), \mathcal{I}_2 and \mathcal{I}_3 are two dimensionless integrals defined in the Appendix A by Eqs. (A30) and (A31), respectively.

We note that the fluctuation pressure is purely attractive; thus, fluctuations lower the free energy. Although the expression Eq. (29) looks complicated, each term, however, has a simple physical interpretation. The first term in Eq. (29) is the pressure arising from counterion fluctuations near the surfaces. In fact, if all of the counterions is condensed $\tau = 1$, we observe that $\mathcal{M}(q)$ in Eq. (A14) becomes $\mathcal{M}(q) = -e^{-qd}/(1 + q\lambda_D)$ and that the only contribution to the pressure in Eq. (29) is the first term, which becomes in this limit

$$\beta \Pi(d) = - \int \frac{d^2 \mathbf{q}}{(2\pi)^2} \frac{q}{e^{2qd}(1 + q\lambda_D)^2 - 1}. \quad (30)$$

This expression is exactly the pressure derived in Ref. [4], arising from 2D fluctuations of the counterions. It scales like $\Pi(d) \sim -1/d^3$ for large distances.

The second term in Eq. (29) may be interpreted as the coupling between the counterions near the surfaces and those in the bulk. This can be seen by considering the asymptotic behavior of the pressure for large d in the no condensate limit $\tau = 0$, *i.e.* the fluctuation corrections to the PB pressure. In this case, in addition to the usual d^{-3} scaling law arising from counterion fluctuations near the surfaces, the second term in Eq. (29) contributes a term, which scales as $\sim d^{-3} \ln(d/\lambda)$ in the large d limit. Therefore, the pressure

$$\Pi(d) \sim -\frac{1}{d^3} - \frac{1}{d^3} \ln(d/\lambda), \quad (31)$$

contains a logarithmic term, which dominates the d^{-3} term for large distances. This term has been obtained by several authors previously [17, 18] and in particular, Ref. [18] shows that this term arises physically from the coupling between counterions near the surfaces and those in the bulk. Therefore, Eq. (29) recovers the PB limit $\tau = 0$ and the 2D limit $\tau = 1$ as special cases. Although the fluctuation corrections to the PB ($\tau = 0$) pressure have been considered previously, we stress that Eq. (29) is a generalization which allows for counterion condensation and may apply to other physical situations, such as ions absorption.

Combining with the mean-field pressure, we obtain the total pressure

$$\beta \Pi_{tot}(d) = \frac{2\alpha^2}{\ell_B} \left\{ 1 - \frac{\ell_B}{8\pi\lambda_R} \frac{(1 + b^2)(\mathcal{I}_2 - \mathcal{I}_3)}{2 + \frac{d}{\lambda_R}(1 + b^2)} \right\} - \int \frac{d^2 \mathbf{q}}{(2\pi)^2} \frac{q \mathcal{M}^2(q)}{1 - \mathcal{M}^2(q)}. \quad (32)$$

The behavior of the total pressure depends on the coupling constant $g \equiv Z^2 \ell_B / \lambda$ and the fraction of condensed counterions $\tau \equiv Zn_c/n_0$. For $g \ll 1$ and $\tau \ll 1$, the fluctuation corrections are small and the total pressure $\Pi_{tot}(d)$ is controlled by the mean-field repulsion. On the other hand, for $\tau \sim 1$ the mean-field repulsion is greatly reduced and the fluctuation attraction can overcome the repulsion at finite distances. Furthermore, for $g \sim 1$ the short distance behavior is highly sensitive to τ : Even a very small number of condensed counterions would turn the total pressure, otherwise repulsive for $\tau = 0$, into attractive for short distances. For $g \gg 1$, the fluctuation attraction becomes dominant at short distances even when there is no condensate, and the effect of finite τ is to push the attractive region out to a larger length scale. Hence, if there is sufficient number of condensed counterions, the pressure is attractive even for large distances. Our next task is to determine the fraction of condensed counterions τ as determined by the minimum of the total free energy.

B. Equilibrium Properties

The equilibrium state of the system is determined by minimizing the total free energy with respect to the order parameter τ . Therefore, we need to evaluate the derivative of the total free energy Eq. (16) with respect to τ . Let us first consider the mean-field contribution. Explicitly differentiating Eq. (24), we obtain

$$\frac{\partial \beta f_0}{\partial \tau} = \frac{2n_0}{Z} \ln(2\lambda/a) - \frac{2n_0}{Z} + \frac{2n_0}{Z} \ln \frac{\tau}{(1 - \tau)^2} - \frac{2n_0}{Z} \ln[1 + b^2], \quad (33)$$

where $\lambda = 4Z/(\ell_B n_0)$ is the “bare” Gouy-Chapman length. To obtain the fluctuation contributions, we again

make use of the exact identity: $\delta \ln \det \hat{\mathbf{X}} = \text{Tr} \hat{\mathbf{X}}^{-1} \delta \hat{\mathbf{X}}$ to evaluate the derivative of the fluctuation free energy in Eq. (25),

$$\frac{\partial \beta \Delta \mathcal{F}}{\partial \tau} = \frac{1}{2\ell_B} \int d^3 \mathbf{x} G_{3d}(\mathbf{x}, \mathbf{x}) \times \frac{\partial}{\partial \tau} \left[\frac{2}{\lambda_D} \sum_{\pm} \delta(z \pm d/2) + \kappa^2 e^{-\varphi(z)} \right]. \quad (34)$$

This expression can be explicitly evaluated using similar techniques outlined in Appendix A and the result is given by

$$\frac{1}{\mathcal{A}} \frac{\partial \beta \Delta \mathcal{F}}{\partial \tau} = \frac{4(1-\tau)}{\lambda^2} \left[\frac{1}{2} \mathcal{I}_1 + \frac{1+b^2}{2} \mathcal{I}_3 + \frac{2b^2 (\mathcal{I}_2 - \mathcal{I}_3)}{2 + \frac{d}{\lambda_R}(1+b^2)} \right], \quad (35)$$

where \mathcal{I}_2 and \mathcal{I}_3 are given in Eqs. (A30) and (A31), respectively, and \mathcal{I}_1 is defined by

$$\mathcal{I}_1[d/\lambda_R] \equiv \int \frac{d^2 \mathbf{q}}{(2\pi)^2} \frac{4\pi\lambda_R}{2q} [\mathcal{G}(d/2) - 1 + \mathcal{L}(q)], \quad (36)$$

where $\mathcal{L}(q)$ and $\mathcal{G}(d/2)$ are defined by Eqs. (A18) and (A19), respectively, in Appendix A. Note that $\mathcal{I}_1[d/\lambda_R]$ is logarithmically divergent (see Appendix A, Eq. (A34)), as in the case for 2D Debye-Huckel theory, which may be regularized by a microscopic cut-off, chosen to be the size of the counterion a . Finally, using Eqs. (33) and (35), the root of the free energy $\partial F(\tau)/\partial \tau = 0$ can be determined numerically. For example, the case of an isolated charged plate can be obtained by taking the limit $d \rightarrow \infty$ in Eqs. (33) and (35), which leads to the following transcendental equation

$$1 + \ln(g\theta/2) + \ln \frac{(1-\tau)^2}{\tau} + g \int_0^{x_c} dx \frac{1 + 2\gamma(1+x)}{(1+x)[1 + (\gamma+x)(1+x)]} = 0, \quad (37)$$

where $x_c = \frac{2\pi}{(1-\tau)g\theta}$ is the microscopic cut-off. The analysis of this equation gives all the features mentioned in Sec. II. As a consistency check, it can be verified that in the limit $d \rightarrow 0$, Eq. (35) gives the fluctuation free energy for an isolated charged surface but with twice of the surface charge density $2en_0$.

V. RESULTS AND DISCUSSION

Let us first discuss the behavior of the order parameter τ at a fixed separation d between the charged surfaces, as summarized in Fig. 2. The behavior of τ as a function g at a finite distance d is qualitatively identical to the case of infinite separation. For weak couplings $g \ll 1$, there is small but finite number of condensed counterions

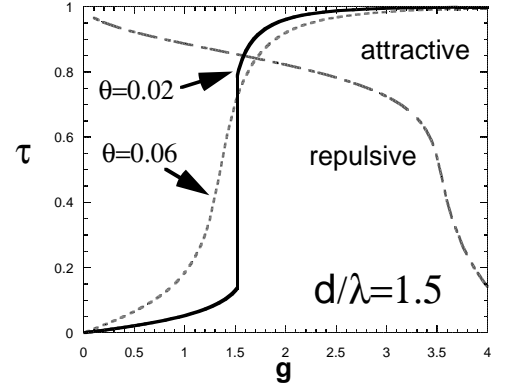


FIG. 2: The fraction of condensed counterions $\tau \equiv Zn_c/n_0$ as a function of $g \equiv Z^2 \ell_B / \lambda$ for different values of $\theta = \frac{a}{Z^2 \ell_B}$. At low surface charge $g \ll 1$, the counterion distribution is well described by PB theory since $\tau \ll 1$. However, at high surface charge, correlation effects leads to a large fraction of counterion condensed. The condensation is first-order for $\theta < \theta_c$ and continuous for $\theta > \theta_c$. The critical point is at $\theta_c \sim 0.017$, $g_c \sim 1.23$, and $\tau_c \sim 0.43$.

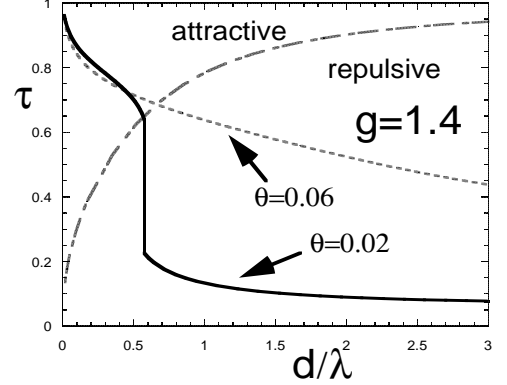


FIG. 3: The fraction of condensed counterions as a function of distance.

but the total pressure remains repulsive. For sufficiently high $g \sim 1$, the condensation proceeds continuously for $\theta > \theta_c$ and via a first-order phase transition for $\theta < \theta_c$ at a particular value of the coupling constant $g_0(d, \theta)$. We note that in this regime, the number of counterion condensation becomes significant. This implies that the mean-field repulsion is drastically reduced and the correlated attractions can overcome the repulsion at finite distance. For $\theta \sim 0.02$, roughly corresponding to divalent counterions at room temperature, we find that the onset of the attraction occurs at $g \sim 1.6$ or surface charge of about one charge per 10 nm^2 at a distance $d = 1.5\lambda \sim 40 \text{ \AA}$. These numbers are order of magnitude consistent with computer simulations [10].

Next, we discuss counterion condensation and the total pressure of system as a function of distance. Note that this scenario is more physically relevant, since surface force experiments usually vary the distance between charged surfaces rather than changing their sur-

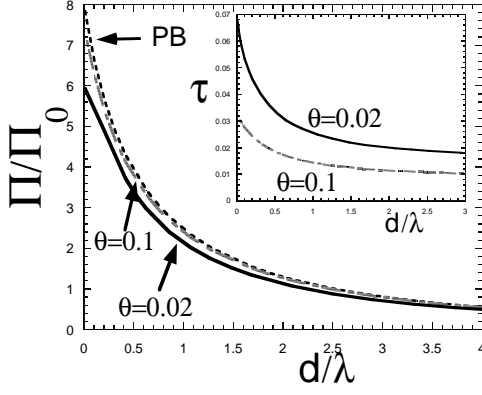


FIG. 4: The pressure profile for monovalent ($\theta = 0.1$) and divalent ($\theta = 0.02$) counterions in the case of low surface charges g .

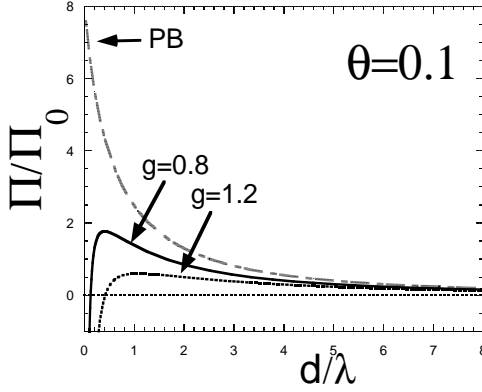


FIG. 5: The pressure profile for monovalent counterions in the case of moderate coupling $g \sim 1$.

face charge densities. For low surface charges $g \ll 1$, as shown in Fig. 4, the counterion condensation is continuous as a function of separation and the fraction of condensed counterion remains small but finite. We note that τ generally increases as the distance of two surfaces decreases, but remains fairly constant up to λ . This is not surprising since there is an entropy loss of the free counterions due to confinement. However, the pressure remains repulsive and shows little difference from the PB pressure profile, as expected.

For sufficiently high coupling $g \sim 1$, we have several interesting regimes depending on the reduced temperature θ (see Fig. 3). For $\theta > \theta_c$, the counterions condense *continuously* as the separation d decreases and the pressure of the system remains repulsive down to very short distances, as shown in Fig. 5, where we have plotted the pressure profile for monovalent counterions ($\theta = 0.1$) for different values of g . Note also that there is still a repulsive barrier, which decreases with increasing g , while the range of the attraction is shifted to larger separations. For $g = 1.2$, corresponding to a surface charge density of about one charge per $\Sigma \sim 300 \text{ \AA}^2$, the total pressure becomes attractive at about $d \sim 10 \text{ \AA}$. It should be noted

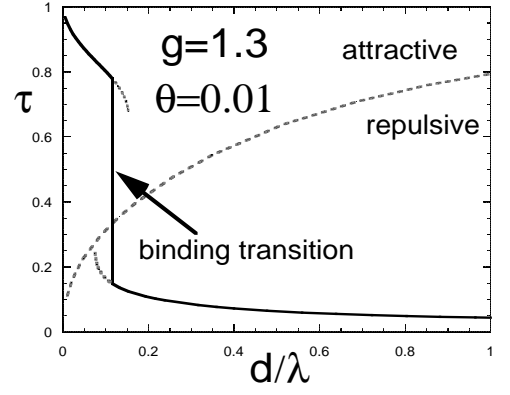


FIG. 6: First-order binding transition: for the case of trivalent counterion ($\theta = 0.01$), the number of condensed counterions (τ) exhibits a discontinuous jump at a particular distance.

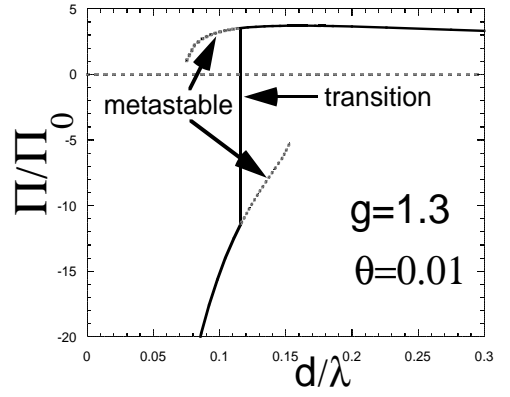


FIG. 7: The pressure profile for the first-order binding transition.

that in real experimental settings, other strong repulsive force, such as hard-core or hydration force, that we have not taken into account in our model, may become important and may overwhelm this correlated attraction at length scale less than $\sim 20 \text{ \AA}$ [1]. This may explain why attraction is difficult to observe experimentally for *monovalent* counterions. Moreover, the pressure profile for large separations is similar to that of the PB theory, except with a renormalized or effective surface charged density. Indeed, it is known experimentally that in order to fit experimental data to the PB theory, it is necessary to use an effective surface charge, which is always lower than the actual surface charge density [1]. Therefore, this counterion condensation picture provides a possible scenario in which this phenomenon can be accounted for theoretically, without invoking charge regulation mechanism.

However, for $\theta < \theta_c$ the behavior of the order parameter τ and the total pressure of the system are qualitatively different (see Fig. 3). We find that there is a range in the coupling constant: $g_\infty(\theta)/2 < g < g_\infty(\theta)$, in which the order parameter displays a finite jump at a particular separation $d_0(g, \theta)$, and the counterion condensation

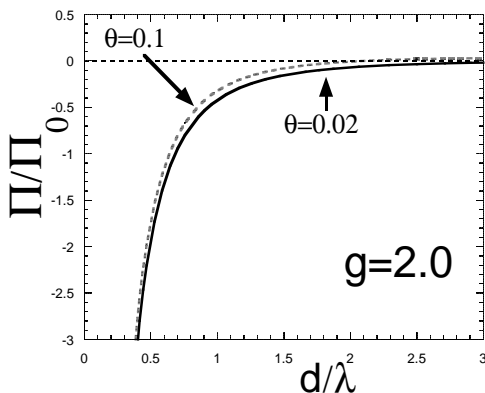


FIG. 8: The pressure profile for high surface charges. Note that the distance at which the pressure turns attractive can be large compared to the Gouy-Chapmann length λ .

is first-order as a function of the separation d . Here, $g_\infty(\theta)$ denotes the coupling constant at which the first-order counterion occurs at infinite separation, *i.e.* an isolated charged plate (see Sec. II and Ref. [14]). Thus, in the limit $g \rightarrow g_\infty(\theta)$, we must have $d_0(g, \theta) \rightarrow \infty$, since the system is composed of two isolated charged plates. On the other hand, we have $d_0(g, \theta) \rightarrow 0$ as $g \rightarrow g_\infty(\theta)/2$, because this limit corresponds to a single charged plate with twice of the surface charge density, *i.e.* $\sigma = 2en_0$. This striking behavior of the order parameter has interesting implications for the interaction for the system. Indeed, for sufficiently short distances, we find that the first-order counterion condensation spontaneously can take the system from the repulsive to the attractive regime, resulting in a novel first-order binding transition. This is illustrated in Fig. 6 for the case of trivalent counterions at room temperature $\theta = 0.01$ at $g = 1.3$, corresponding to a surface density of one charge per $\Sigma \sim 70 \text{ nm}^2$. (For trivalent counterions, the first-order counterion condensation occurs in the range of $0.9 < g < 1.8$ [14].) The corresponding pressure profile is plotted in Fig. 7, which shows that the binding transition occurs at about $d \sim 10 \text{ \AA}$. We note that an interesting consequence of this first-order binding transition is the existence of metastable states, which may have important manifestations in surface force experiments. It is easy to imagine that the system can be trapped in different metastable states, and therefore, hysteresis may occur as the two surfaces are pushing in and pulling out again. Indeed, there are some experimental support for this behavior for multivalent counterions in similar systems [31]. It is important to emphasize that this interesting behavior is not included in the mean-field PB theory. Note also that this first-order binding transition can only take place at short distances. This is because $d_0(g, \theta)$ generally increases with increasing g , and eventually when g is near $g_\infty(\theta)$, the condensation occurs within the repulsive regime and the binding transition becomes continuous. Thus, direct experimental observation of the first-order binding transition may prove subtle.

Finally, For $g > g_\infty(\theta)$ and $\theta < \theta_c$, the condensation again becomes continuous. This is because the first-order phase transition has already occurred at infinite separation, in which $\tau \sim 1$. In this regime, the length scale at which the attraction starts to overcome the repulsion can be quite large (see Fig. 8). In the case of divalent counterions, we find that the onset of attraction occurs at $d \sim 100 \text{ \AA}$. Clearly, the higher the surface charge or g , we have longer the range of the attraction; therefore, together with the mechanism of fluctuation-driven counterion condensation, the correlated attraction may explain the long-ranged attractions observed experimentally. Moreover, we note that there is a qualitative change in the shape of the pressure: the repulsive barrier disappears. This may mark an onset of the aggregation and has important experimental manifestations on the phase behavior of the macroions.

In summary, by incorporating the condensation driven by fluctuations, we show that the net pressure between two similarly charged surfaces becomes negative, hence attractions, at a length scale much longer than the Gouy-Chapmann length. We also predict several distinct behaviors of the system, depending on the valence of the counterions, that deviates significantly from the classical theory of the double-layer interactions. While our calculation is based on the Gaussian fluctuation theory which may break down for very high surface charge density, a complementary treatment is considered by Shklovskii [6] in this regime, where the condensed counterions are assumed to form a 2D Strongly Correlated Liquid. That theory predicts a strongly reduced surface charge and exponentially large renormalized Gouy-Chapmann length, qualitatively similar to our results that for high surface charge most of the counterions are condensed. Moreover, it was shown in Ref. [20] that by perturbing around the low temperature Wigner crystal ground state, the long-ranged attraction persists to be operative, independent of the ground state. Thus, at large distances, we believe that our picture should capture the interaction of two similarly charged surfaces in the regime between where PB theory is appropriate (low surface charge) and the strong coupling limit [6, 32].

However, there remain fundamental issues to be addressed in the future. For example, in real systems, the charged surfaces are often characterized by discrete surface charge distribution. In recent studies [33], it is shown that the counterion distribution is strongly modified if discreteness is taken into account. In particular, the counterions tend to be more “localized” near the charged surface. It remains to be seen how this affects the condensation picture presented in this paper; it is possible that this effect may smooth out the first-order transition. However, we believe that a rapid variation of the condensation reflecting the first-order transition should remain.

Acknowledgments

We wish to acknowledge J.-F. Joanny, D.B. Lukatsky, T.C. Lubensky, S.A. Safran, and P. Sen for important discussions. A.W.C.L. would like to thank Prof. P.-G. de Gennes for fruitful discussions and for a wonderful hospitality at Collège de France, Paris where most of this work is completed. PP acknowledges support from grants MRL-NSF-DMR-0080034 and NSF-DMR-9972246. A.W.C.L. acknowledges support from NIH un-

der Grant No. HL67286.

APPENDIX A: DERIVATION OF THE FLUCTUATION PRESSURE

In this appendix, we present a detail derivation of the pressure arising from fluctuations. The derivative of the fluctuation free energy with respect to the distance d is given in Eq. (27)

$$\frac{\partial \beta \Delta \mathcal{F}}{\partial d} = \frac{1}{2\ell_B} \int d^3 \mathbf{x} G_{3d}(\mathbf{x}, \mathbf{x}) \frac{\partial}{\partial d} \left[\frac{2}{\lambda_D} \sum_{\pm} \delta(z \pm d/2) + \kappa^2 e^{-\varphi(z)} \right], \quad (\text{A1})$$

where $\kappa^2 e^{-\varphi(z)} = 2\alpha^2 \sec^2(\alpha z) \Theta(z) + 2(|z| - d/2 + \xi)^{-2} \tilde{\Theta}(z)$ as defined in Eq. (26), $\xi \equiv \lambda_R/(1+b^2)$, and $G_{3d}(\mathbf{x}, \mathbf{x}')$ is the Green's function defined as the inverse operator of $\hat{\mathbf{K}}_{3d}$ and satisfies the equation Eq. (28), which in Fourier space can be written as:

$$\left[-\frac{\partial^2}{\partial z^2} + q^2 + \frac{2}{\lambda_D} \sum_{\pm} \delta(z \pm d/2) + \kappa^2 e^{-\varphi(z)} \right] G_{3d}(z, z'; q) = \ell_B \delta(z - z').$$

The Green's function can be solved by standard technique [34]; first, we note that the homogeneous solutions are given by

$$h_{\pm}^{\leq}(z; q) = e^{\pm qz} \left[1 \pm \frac{\alpha}{q} \tan(\alpha z) \right], \quad (\text{A2})$$

for $|z| < d/2$ and

$$h_{\pm}^{\geq}(z; q) = e^{\pm q|z|} \left[1 \mp \frac{1}{q(|z| - d/2 + \xi)} \right], \quad (\text{A3})$$

for $|z| > d/2$. We have two cases to consider: $|z'| < d/2$ and $|z'| > d/2$. In the former case, we split the space into four regions: $z < -d/2$, $-d/2 < z < z'$, $z' < z < d/2$, and $z > d/2$ and write

$$G_{-}(z, z'; q) = A(z') h_{+}^{\geq}(z; q), \quad \text{for } z < -d/2, \quad (\text{A4})$$

$$G_{<}(z, z'; q) = B(z') h_{+}^{\leq}(z; q) + C(z') h_{-}^{\leq}(z; q), \quad \text{for } -d/2 < z < z', \quad (\text{A5})$$

$$G_{>}(z, z'; q) = D(z') h_{+}^{\leq}(z; q) + E(z') h_{-}^{\leq}(z; q), \quad \text{for } z' < z < d/2, \quad (\text{A6})$$

$$G_{+}(z, z'; q) = F(z') h_{-}^{\geq}(z; q), \quad \text{for } z > d/2. \quad (\text{A7})$$

The coefficients $A(z') \dots F(z')$ are determined by the following boundary conditions

$$G_{3d}(\pm d/2, z'; q) = G_{3d}(\pm d/2, z'; q), \quad (\text{A8})$$

$$\partial_z G_{3d}(z, z'; q)|_{z=\pm d/2} - \partial_z G_{3d}(z, z'; q)|_{z=\pm d/2} = (2/\lambda_D) G_{3d}(\pm d/2, z'; q), \quad (\text{A9})$$

$$G_{3d}(z', z'; q) = G_{3d}(z', z'; q), \quad (\text{A10})$$

$$\partial_z G_{3d}(z, z'; q)|_{z=z'} - \partial_z G_{3d}(z, z'; q)|_{z=z'} = \ell_B. \quad (\text{A11})$$

After some algebra, we obtain specifically

$$E(z') = \frac{\ell_B}{2q} \frac{h_{+}^{\leq}(z') + \mathcal{M}(q) h_{-}^{\leq}(z')}{(1 + \alpha^2/q^2) [1 - \mathcal{M}^2(q)]}, \quad (\text{A12})$$

$$D(z') = \mathcal{M}(q) E(z'), \quad (\text{A13})$$

$$\mathcal{M}(q) = \frac{e^{-qd} [(1+b^2)^2 + \gamma(1-b^2 - q\lambda_R)(1+b^2 + q\lambda_R)]}{(1+b^2)^2(1+q\lambda_R) + (\gamma + q\lambda_R)(1+b^2 + q\lambda_R)(1-b^2 + q\lambda_R)}, \quad (\text{A14})$$

where $\gamma \equiv \lambda_R/\lambda_D = 2\tau/(1-\tau)$. Therefore, the Green's function $G_{3d}(\mathbf{x}, \mathbf{x})$ for $|z| \leq d/2$ is explicitly given by

$$G_{3d}^{<}(\mathbf{x}, \mathbf{x}) = \int \frac{d^2\mathbf{q}}{(2\pi)^2} \frac{\ell_B}{2q} \left\{ \frac{1 + \mathcal{M}^2(q)}{1 - \mathcal{M}^2(q)} - \frac{\alpha^2}{q^2} \frac{\sec^2(\alpha z)}{1 + \alpha^2/q^2} \frac{1 + \mathcal{M}^2(q)}{1 - \mathcal{M}^2(q)} \right. \quad (\text{A15})$$

$$\left. + \frac{2\mathcal{M}(q)}{1 - \mathcal{M}^2(q)} \left[\frac{[1 + \alpha^2/q^2 \tan^2(\alpha z)] \cosh(2qz) + 2\alpha/q \tan(\alpha z) \sinh(2qz)}{1 + \alpha^2/q^2} \right] \right\}. \quad (\text{A16})$$

Note that the Green's function is symmetric with respect to z , as expected from the symmetry of the problem. Similar calculation can be done for the case $|z| \geq d/2$ and the result is

$$G_{3d}^{>}(\mathbf{x}, \mathbf{x}) = \int \frac{d^2\mathbf{q}}{(2\pi)^2} \frac{\ell_B}{2q} \left\{ 1 - \frac{1 - \mathcal{L}(q) e^{-2q(|z| - d/2)} [1 + q(|z| - d/2 + \xi)]^2}{q^2(|z| - d/2 + \xi)^2} \right\}, \quad (\text{A17})$$

where $\mathcal{L}(q)$ is given by

$$\mathcal{L}(q) = \frac{e^{-qd} \mathcal{G}(d/2)}{[h_+^>(d/2)]^2} - \frac{h_+^>(d/2) e^{-qd}}{h_+^>(d/2)}, \quad (\text{A18})$$

and

$$\mathcal{G}(d/2) \equiv \frac{[h_+^<(d/2) + \mathcal{M}(q) h_-^<(d/2)][h_-^<(d/2) + \mathcal{M}(q) h_+^<(d/2)]}{(1 + \alpha^2/q^2)[1 - \mathcal{M}^2(q)]} = \frac{2q}{\ell_B} G_{3d}[d/2, d/2; q]. \quad (\text{A19})$$

Returning to the expression in Eq.(A1), we note that it can be separated into three parts:

$$\frac{1}{\mathcal{A}} \frac{\partial \beta \Delta \mathcal{F}_A}{\partial d} = \frac{2}{\ell_B \lambda_D} \int \frac{d^2\mathbf{q}}{(2\pi)^2} \int_0^\infty dz G_{3d}(z, z; q) \frac{\partial}{\partial d} \delta(z - d/2), \quad (\text{A20})$$

$$\frac{1}{\mathcal{A}} \frac{\partial \beta \Delta \mathcal{F}_B}{\partial d} = \frac{1}{\ell_B} \int \frac{d^2\mathbf{q}}{(2\pi)^2} \int_0^\infty dz G_{3d}(z, z; q) \Theta(z) \frac{\partial}{\partial d} [2\alpha^2 \sec^2(\alpha z)], \quad (\text{A21})$$

$$\frac{1}{\mathcal{A}} \frac{\partial \beta \Delta \mathcal{F}_C}{\partial d} = \frac{1}{\ell_B} \int \frac{d^2\mathbf{q}}{(2\pi)^2} \int_0^\infty dz G_{3d}(z, z; q) \tilde{\Theta}(z) \frac{\partial}{\partial d} \left[\frac{2}{(z - d/2 + \xi)^2} \right], \quad (\text{A22})$$

where we have used the fact that the integrand is symmetric with respect to z . Note also that there should also be two terms containing $\partial \Theta(z)/\partial d$ and $\partial \tilde{\Theta}(z)/\partial d$ in $\partial \beta \Delta \mathcal{F}_B/\partial d$ and $\partial \beta \Delta \mathcal{F}_C/\partial d$, respectively; however, they cancel identically when they are added together.

Let us first discuss Eq. (A20); using the identity: $\frac{\partial}{\partial d} \delta(z - d/2) \equiv -\frac{1}{2} \frac{\partial}{\partial z} \delta(z - d/2)$, and integrating by part, it can be transformed into

$$\frac{1}{\mathcal{A}} \frac{\partial \beta \Delta \mathcal{F}_A}{\partial d} = \frac{1}{\ell_B \lambda_D} \int \frac{d^2\mathbf{q}}{(2\pi)^2} \frac{\partial G_{3d}(z, z; q)}{\partial z} \Big|_{z=d/2+}. \quad (\text{A23})$$

Using the boundary condition in Eq. (A9)

$$\partial_z G_{3d}(z, z; q)|_{z=d/2+} = \partial_z G_{3d}(z, z; q)|_{z=d/2-} + (2/\lambda_D) G_{3d}(d/2, d/2; q),$$

and the explicit expression for the Green's function given in Eq. (A16), we obtain after some algebra

$$\begin{aligned} \frac{1}{\mathcal{A}} \frac{\partial \beta \Delta \mathcal{F}_A}{\partial d} &= \frac{1}{\ell_B \lambda_D} \int \frac{d^2\mathbf{q}}{(2\pi)^2} \frac{\ell_B}{2q} \frac{2}{\lambda_D} \left\{ \frac{-\mathcal{M}^2(q)}{1 - \mathcal{M}^2(q)} \frac{q\lambda_D(1+b^2)^2(b^2 + q\lambda_R + q\lambda_D)}{(1+b^2)^2 + \gamma(1-b^2 - q\lambda_R)(1+b^2 + q\lambda_R)} \right. \\ &+ \frac{q\lambda_D}{1 - \mathcal{M}^2(q)} \frac{b^2(1+b^2)^2}{(1+b^2)^2(1+q\lambda_R) + (\gamma + q\lambda_R)(1+b^2 + q\lambda_R)(1-b^2 + q\lambda_R)} \left. \right\} \\ &+ \int \frac{d^2\mathbf{q}}{(2\pi)^2} \frac{q\mathcal{M}^2(q)}{1 - \mathcal{M}^2(q)}. \end{aligned} \quad (\text{A24})$$

The next term, Eq. (A21), can be shown to be

$$\frac{1}{\mathcal{A}} \frac{\partial \beta \Delta \mathcal{F}_B}{\partial d} = -\frac{8}{\ell_B \lambda_R^2} \frac{(1+b^2)b}{2 + \frac{d}{\lambda_R}(1+b^2)} \int \frac{d^2\mathbf{q}}{(2\pi)^2} \int_0^{\alpha d/2} dx G_{3d}(x, x; q) \sec^2 x (1 + x \tan x). \quad (\text{A25})$$

In evaluating the x -integral, we note that there is a nontrivial integral which involves the last term inside the bracket of Green's function in Eq. (A16); it reads

$$\mathcal{Q} = \int_0^{\tilde{d}} dx \sec^2 x (1 + x \tan x) \left\{ \left[1 + (2/k)^2 \tan^2 x \right] \cosh kx + 4/k \tan x \sinh kx \right\},$$

where $k \equiv 2q/\alpha$ and $\tilde{d} \equiv \alpha d/2$. Note that none of these integrals can be expressed in terms of elementary functions, but integrating by parts several times, one can show that the integral \mathcal{Q} can be expressed in closed form with the help of the relation: $2b \tan(\alpha d/2) = 1 - b^2$, by

$$\begin{aligned} \mathcal{Q} = & \frac{(1-b^2)^2(1+b^2)}{16b(q\lambda_R)^2} \left[2 + \frac{d}{\lambda_R} (1+b^2) \right] \cosh(qd) - \frac{b(1+b^2)}{4(q\lambda_R)^2} \left[2 + \frac{d}{\lambda_R} (1+b^2) \right] \cosh(qd) \\ & - \frac{(1-b^2)^2b}{4(q\lambda_R)^2} \cosh(qd) + \frac{b \cosh(qd)}{(q\lambda_R)^2} + \frac{(1-b^2)(1+b^2)}{8b(q\lambda_R)} \left[2 + \frac{d}{\lambda_R} (1+b^2) \right] \sinh(qd) \\ & + \frac{b(1+b^2)}{2(q\lambda_R)} \sinh(qd). \end{aligned}$$

Substituting this result back into Eq. (A25) and rearranging terms, we obtain

$$\begin{aligned} \frac{1}{\mathcal{A}} \frac{\partial \beta \Delta \mathcal{F}_B}{\partial d} = & -\frac{(1+b^2)^2}{\ell_B \lambda_R^2} \int \frac{d^2 \mathbf{q}}{(2\pi)^2} \frac{\ell_B}{2q} \left[\frac{\mathcal{G}(d/2)}{2} + \mathcal{J}(d/2) \right] + \frac{1}{\ell_B \lambda_R^2} \frac{4b^2(1+b^2)}{2 + \frac{d}{\lambda_R}(1+b^2)} \times \\ & \int \frac{d^2 \mathbf{q}}{(2\pi)^2} \frac{\ell_B}{2q} \left[\frac{\mathcal{G}(d/2)}{2} + \mathcal{J}(d/2) + \frac{2(1-b^2)\mathcal{J}(d/2)}{(q\lambda_R)^2(1+\alpha^2/q^2)} - \frac{2}{q\lambda_R} \frac{2\mathcal{M}(q) \sinh(qd)}{(1+\alpha^2/q^2)[1-\mathcal{M}^2(q)]} \right] \end{aligned}$$

where $\mathcal{J}(d/2)$ is defined by the expression

$$\mathcal{J}(d/2) \equiv \frac{1}{2} \left[\frac{1 + \mathcal{M}^2(q)}{1 - \mathcal{M}^2(q)} - \frac{2\mathcal{M}(q) \cosh qd}{1 - \mathcal{M}^2(q)} \right]. \quad (\text{A26})$$

Finally, we turn to the last term in Eq. (A1), Eq. (A22). With the help of the integral

$$\int_{d/2}^{\infty} dz \frac{G_{3d}(z, z; q)}{(z - d/2 + \xi)^3} = \frac{\ell_B (1+b^2)^2}{2q} \left[\frac{1}{2} \mathcal{G}(d/2) + \frac{1}{2} - \frac{1}{2} \mathcal{L}(q) \right], \quad (\text{A27})$$

Eq. (A22) can be written as

$$\begin{aligned} \frac{1}{\mathcal{A}} \frac{\partial \beta \Delta \mathcal{F}_C}{\partial d} = & \frac{(1+b^2)^2}{\ell_B \lambda_R^2} \int \frac{d^2 \mathbf{q}}{(2\pi)^2} \frac{\ell_B}{2q} \left[\frac{\mathcal{G}(d/2) + 1 - \mathcal{L}(q)}{2} \right] \\ & - \frac{4b^2(1+b^2)}{2 + \frac{d}{\lambda_R}(1+b^2)} \int \frac{d^2 \mathbf{q}}{(2\pi)^2} \frac{\ell_B}{2q} \left[\frac{\mathcal{G}(d/2) + 1 - \mathcal{L}(q)}{2} \right], \end{aligned} \quad (\text{A28})$$

which can be combined with the expression for $\partial \beta \Delta \mathcal{F}_B / \partial d$ above (note that $\mathcal{G}(d/2)$ cancels nicely) to yield

$$\frac{1}{\mathcal{A}} \frac{\partial \beta \Delta \mathcal{F}_{B+C}}{\partial d} = \frac{(1+b^2)^2}{\ell_B \lambda_R^2} \frac{\ell_B}{4\pi\lambda_R} \mathcal{I}_3 + \frac{1}{\ell_B \lambda_R^2} \frac{4b^2(1+b^2)}{2 + \frac{d}{\lambda_R}(1+b^2)} \frac{\ell_B}{4\pi\lambda_R} (\mathcal{I}_2 - \mathcal{I}_3), \quad (\text{A29})$$

where we have defined the following dimensionless integrals

$$\mathcal{I}_2 \equiv \int \frac{d^2 \mathbf{q}}{(2\pi)^2} \frac{4\pi\lambda_R}{2q} \left[\frac{2(1-b^2)\mathcal{J}(d/2)}{(q\lambda_R)^2(1+\alpha^2/q^2)} - \frac{2}{q\lambda_R} \frac{2\mathcal{M}(q) \sinh(qd)}{(1+\alpha^2/q^2)[1-\mathcal{M}^2(q)]} \right], \quad (\text{A30})$$

$$\mathcal{I}_3 \equiv \int \frac{d^2 \mathbf{q}}{(2\pi)^2} \frac{4\pi\lambda_R}{2q} \left[\frac{1}{2} - \frac{1}{2} \mathcal{L}(q) - \mathcal{J}(d/2) \right]. \quad (\text{A31})$$

With some straightforward but tedious algebra, they can be cast into more explicit form:

$$\begin{aligned} \mathcal{I}_2[d/\lambda_R] = & \int_0^{\infty} dx \frac{2x \left[(1-b^2+x)^2 + \gamma(1+b^2+x)(1-b^2+x) - b^2(4b^2+x^2) \right]}{(4b^2+x^2)[1-\mathcal{M}^2(x)][(1+b^2)^2(1+x) + (\gamma+x)(1+b^2+x)(1-b^2+x)]} \\ & - \int_0^{\infty} dx \frac{2x\mathcal{M}^2(x) \left\{ (1-b^2-x)[(1-b^2+x) + \gamma(1+b^2+x)] - (b^2+x)(4b^2+x^2) \right\}}{(4b^2+x^2)[1-\mathcal{M}^2(x)][(1+b^2)^2 + \gamma(1-b^2-x)(1+b^2+x)]}, \end{aligned} \quad (\text{A32})$$

and

$$\begin{aligned} \mathcal{I}_3[d/\lambda_R] = & - \int_0^\infty dx \frac{2\gamma x b^2}{[1 - \mathcal{M}^2(x)] [(1+b^2)^2(1+x) + (\gamma+x)(1+b^2+x)(1-b^2+x)]} \\ & + \int_0^\infty dx \frac{2x\mathcal{M}^2(x) [x + \gamma(b^2+x)]}{[1 - \mathcal{M}^2(x)] [(1+b^2)^2 + \gamma(1-b^2-x)(1+b^2+x)]}, \end{aligned} \quad (\text{A33})$$

where we have made a change of the integration variable $x = q\lambda_R$. Now, observe that the first term in Eq. (A29) cancels precisely the first term in Eq. (A24). Therefore, combining the two expressions, we obtain Eq. (29) for the fluctuation pressure. Similarly, $\mathcal{I}_1[d/\lambda_R]$ defined in Eq. (36) can be expressed as:

$$\begin{aligned} \mathcal{I}_1[d/\lambda_R] = & - \int \frac{d^2\mathbf{q}}{(2\pi)^2} \frac{4\pi\lambda_R}{2q} \frac{q\lambda_R [(1+b^2)^2 + 2\gamma(1-b^2+q\lambda_R)]}{(1+b^2)^2(1+q\lambda_R) + (\gamma+q\lambda_R)(1+b^2+q\lambda_R)(1-b^2+q\lambda_R)} \\ & - \int \frac{d^2\mathbf{q}}{(2\pi)^2} \frac{4\pi\lambda_R}{2q} \frac{q\lambda_R\mathcal{M}^2(q)}{1-\mathcal{M}^2(q)} \left\{ \frac{(1+b^2)^2 + 2\gamma(1-b^2+q\lambda_R)}{(1+b^2)^2(1+q\lambda_R) + (\gamma+q\lambda_R)(1+b^2+q\lambda_R)(1-b^2+q\lambda_R)} \right. \\ & \left. - \frac{(1+b^2)^2 + 2q\lambda_R(1-b^2) + 2(q\lambda_R)^2 + 2\gamma(1-b^2-q\lambda_R)}{(1+b^2)^2 + \gamma(1-b^2-q\lambda_R)(1+b^2+q\lambda_R)} \right\}. \end{aligned} \quad (\text{A34})$$

Note that the first term in this expression is logarithmically divergent.

-
- [1] J.N. Israelachvili, *Intermolecular and Surface Forces*. (Academic Press Inc., San Diego, 1992); W.M. Gelbart, R.F. Bruinsma, P.A. Pincus, and V.A. Parsegian, *Physics Today* **53**, 38 (2000).
- [2] I. Rouzina and V.A. Bloomfield, *J. Phys. Chem.* **100**, 9977 (1996); J. Arenzon, J.F. Stilck, and Y. Levin, *Eur. Phys. J. B.* **12**, 79 (1999); B.I. Shklovskii, *Phys. Rev. E* **60**, 5082 (1999).
- [3] B.-Y. Ha and A. J. Liu, *Phys. Rev. Lett.* **79**, 1289 (1997); *Phys. Rev. Lett.* **81**, 1011 (1998); *Phys. Rev. E* **58**, 6281 (1998); *Phys. Rev. E* **60**, 803 (1999).
- [4] P. Pincus and S.A. Safran, *Europhys. Lett.* **42**, 103 (1998).
- [5] R. Netz and H. Orland, *Eur. Phys. J. E* **1**, 203 (2000).
- [6] V.I. Perel and B.I. Shklovskii, *Physica A* **274**, 446 (1999); T.T. Nguyen, A.Yu. Grosberg, and B.I. Shklovskii, *Phys. Rev. Lett.* **85**, 1568 (2000).
- [7] R. Kjellander, S. Marcelja, and J.P. Quirk, *J. Colloid Interface Sci.* **126**, 194 (1988); H. Wennerstrom, A. Khan, and B. Lindman, *Adv. Colloid Interface Sci.* **34**, 433 (1991); V.A. Bloomfield, *Biopolymers* **31**, 1471 (1991); R. Podgornik, D. Rau, and V.A. Parsegian, *Biophys. J.* **66**, 962 (1994).
- [8] Patrick Kekicheff and Olivier Spalla, *Phys. Rev. Lett.* **75**, 1851 (1995).
- [9] A.E. Larsen and D.G. Grier, *Nature* **385**, 230 (1997).
- [10] L. Guldbrand, B. Jönsson, H. Wennerström, and P. Linse, *J. Chem. Phys.* **80**, 2221 (1984).
- [11] M.J. Stevens and K. Kremer, *J. Chem. Phys.* **103**, 1669 (1995); N. Grønbech-Jensen, R. J. Mashl, R.F. Bruinsma, and W.M. Gelbart, *Phys. Rev. Lett.* **78**, 2477 (1997); N. Grønbech-Jensen, K.M. Beardmore, and P. Pincus, *Physica A* **261**, 74 (1998).
- [12] R. Messina, C. Holm, and K. Kremer, *Phys. Rev. Lett.* **85**, 872 (2000); *Europhys. Lett.* **51**, 461 (2000).
- [13] J.C. Neu, *Phys. Rev. Lett.* **82**, 1072 (1999); J.E. Sader and D.Y. Chan, *J. Colloid Interface Sci.* **213**, 268 (1999).
- [14] A.W.C. Lau, D.B. Lukatsky, P. Pincus, and S.A. Safran, *Phys. Rev. E* **65**, 051502 (2002).
- [15] R. Kjellander and S. Marcelja, *Chem. Phys. Lett.* **112**, 49 (1984); *J. Phys. Chem.* **90**, 1230 (1986).
- [16] M.J. Stevens and M.O. Robbins, *Europhys. Lett.* **12**, 81 (1990); A. Diehl, M.N. Tamashiro, M.C. Barbosa, and Y. Levin, *Physica A* **274**, 433 (1999).
- [17] Phil Attard, Roland Kjellander, and D. John Mitchell, *Chem. Phys. Lett.* **139**, 219 (1987); P. Attard, D.J. Mitchell, and B.W. Ninham, *J. Chem. Phys.* **88**, 4987 (1988); R. Podgornik, *J. Phys. A* **23**, 275 (1990).
- [18] D.B. Lukatsky and S.A. Safran, *Phys. Rev. E* **60**, 5848 (1999).
- [19] A. Gopinathan, T. Zhou, S.N. Coppersmith, L.P. Kadanoff, and D.G. Grier, *Europhys. Lett.* **57**, 451 (2002).
- [20] A.W.C. Lau, Dov Levine, and P. Pincus, *Phys. Rev. Lett.* **84**, 4116 (2000); A.W.C. Lau, P. Pincus, Dov Levine, and Herb Fertig, *Phys. Rev. E* **63**, 051604 (2001).
- [21] B.-Y. Ha, *Phys. Rev. E* **64**, 031507 (2002).
- [22] T.M. Squires and M.P. Brenner, *Phys. Rev. Lett.* **85**, 4976 (2000).
- [23] M.N. Tamashiro and P. Pincus, *Phys. Rev. E* **60**, 6549 (1999).
- [24] Ning Ma, S.M. Girvin, and R. Rajaramann, *Phys. Rev. E* **63**, 021402 (2001).
- [25] S.A. Safran, *Statistical Thermodynamics of Surfaces, Interfaces, and membranes* (Addison-Wesley Publishing Com., Reading, 1994).
- [26] Alexander L. Fetter, *Phys. Rev. B* **10**, 3739 (1974); H.

- Totsuji, J. Phys. Soc. Japan **40**, 857 (1976); E.S. Velazquez and L. Blum, Physica A **244**, 453 (1997); A.W.C. Lau and P. Pincus, Phys. Rev. Lett. **81**, 1338 (1998).
- [27] L.D. Landau and E.M. Lifshitz, *Statistical Physics*, (Pergamon, New York, 1980), 3rd ed., rev. and enl. by E.M. Lifshitz and L.P. Pitaevskii.
- [28] Note that this is the case where the counterions can be squeezed out of the surfaces, where the density at the mid-plane for $d \ll \lambda$, $\rho_0(0) \sim 1/(l_B \lambda^2)$, instead of $\rho_0(0) \sim 1/(l_B \lambda d)$ where counterions are confined between two charged hard walls.
- [29] J. Hubbard, Phys. Rev. Lett. **3**, 77 (1959); R.L. Stratonovitch, Dokl. Akad. Nauk USSR **115**, 1907 (1957).
- [30] S. Samuel, Phys. Rev. D **18**, 1916 (1978). See also Ref. [5].
- [31] Uri Raviv, private communications; preprint (2001).
- [32] André G. Moreira and R. Netz, Phys. Rev. Lett. **87**, 078301 (2001).
- [33] D.B. Lukatsky, S.A. Safran, A.W.C. Lau, and P. Pincus, Europhys. Lett. **58**, 785 (2002); André G. Moreira and R. Netz, Europhys. Lett. **57**, 911 (2002).
- [34] G. Arfken, *Mathematical Methods for Physicists* (Academic press, Inc., San Diego, 1996).